

Supporting Information

An RGB Color-Tunable Turn-On Electrofluorochromic Device and its Potential for Information Encryption

Xiaojun Wang,^{a, b} Wen Li,^{a, b} Wanru Li,^b Chang Gu,^b Hongzhi Zheng,^b Yuyang Wang,^{a, b} Yu-Mo Zhang,^{*b} Minjie Li,^{a, b} and Sean Xiao-An Zhang^{*a, b}

a. State Key Lab of Supramolecular Structure and Materials, Jilin University, Changchun, 130012, P. R. China. E-mail: seanzhang@jlu.edu.cn

b. College of Chemistry, Jilin University, Changchun, 130012, P. R. China. E-mail: zhangyumo@jlu.edu.cn

Contents

1. General experimental details.....	3
2. The measurement methods of spectroelectrochemistry	5
3. The preparation methods of the solid electrofluorochromic device.....	6
4. Synthesis of the G molecule and R molecule.....	8
5. pH-sensitive fluorescence properties in solution	9
6. Spectroelectrochemical measurements in situ	16
7. Supplementary Figures for solid devices	20
8. NMR spectra.	23
References	25

1. General experimental details

Characterization

¹H NMR and ¹³C NMR spectra were recorded by a Bruker 500M NMR spectrometer. Chemical shift values are given relative to TMS. LC-HRMS analysis was performed on an Agilent 1290-microTOF-Q II mass spectrometer. The melting points were determined using a SGW X-4B microscopy melting point apparatus (Shanghai) and were uncorrected. The UV-Vis absorption spectra were obtained with a Shimadzu UV-2550 double-beam spectrophotometer. Fluorescence spectra were obtained with a Shimadzu spectrofluorimeter RF-5301PC.

Reagents

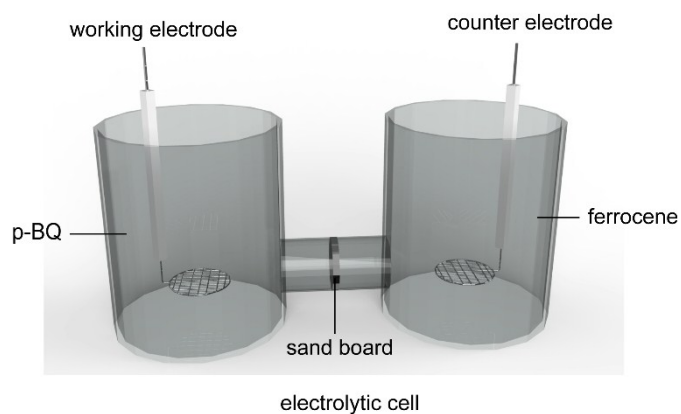
2-(4-Diethylamino-2-hydroxybenzoyl)benzoic acid (98 %, Energy Chemical), resorcinol (99 %, Energy Chemical), trifluoroacetic acid (99 %, Energy Chemical), (2,6-Dimethyl-4H-pyran-4-ylidene)malononitrile (98 %, TCI), p-hydroxybenzaldehyde (99 %, Energy Chemical), Polymethylmethacrylate (PMMA, Energy Chemical), p-Benzoquinone (99 %, Aladdin Reagent Company), ferrocene (99 %, Aladdin Reagent Company) and 7-hydroxycoumarin (98 %, Energy Chemical) were used without further purified. Tetrabutylammonium hexafluorophosphate (TBAPF₆) (98 %, Aladdin Reagent Company) was recrystallized three times in ethanol and dried under vacuum overnight at 80 °C.

Electrochemistry

Cyclic voltammetry (CV) experiments were performed using a Bio-logic electrochemical workstation. Electrochemical experiments were conducted using three-electrode system in chromatographic grade acetonitrile containing TBAPF₆ (0.1 mol/L) as supporting electrolyte. The three-electrode cell consisted of a glass-carbon working electrode (3 mm dia., Chenhua, China), a Pt wire counter electrode (ida, China) and an Ag wire reference electrode (ida, China). The surface of the working electrode was polished with 0.3 and 0.05 μm alumina (ida, China) followed by ultrasonic cleaning in deionized water for three times.

Preparation of $p\text{-BQ}^{\cdot-}$ by electrolysis

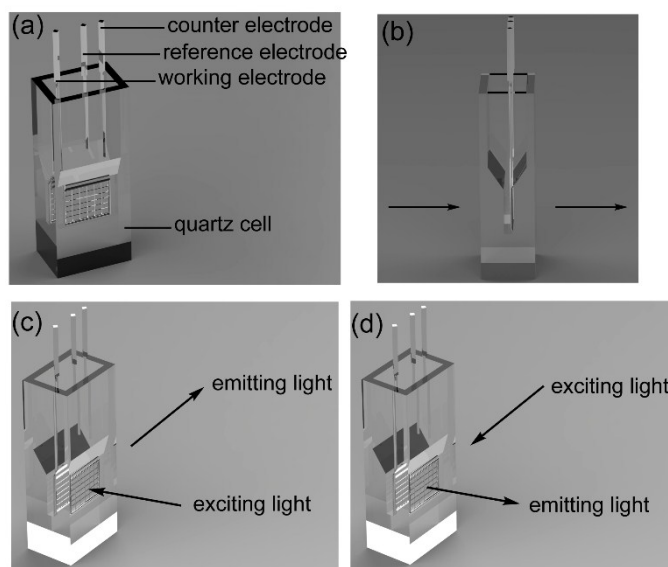
The electrolytic cell was used to produce the *p*-benzoquinone radical anion ($p\text{-BQ}^{\cdot-}$). The *p*-BQ (1.0×10^{-2} M) and TBAPF_6 (0.1 M) in CH_3CN was used as working electrolyte. The ferrocene (1.0×10^{-2} M) and TBAPF_6 (0.1 M) in CH_3CN was used as counter electrolyte to balance the charge. The reaction was stirred under -2 V voltage for 3 h.



Scheme S1 (a) The diagram of electrolytic cell for producing *p*-benzoquinone radical anion ($p\text{-BQ}^{\cdot-}$).

2. The measurement methods of spectroelectrochemistry

A thin-layer (1 mm) quartz glass electrochemical cell (ida, China) (Scheme S2) was used to measure spectroelectrochemical spectra. The three electrodes are consisted of a Pt network working electrode, a Pt wire counter electrode and a Ag/AgNO₃ reference electrode.



Scheme S2 (a) The diagram of the thin-layer quartz electrochemical cell which is used to measure the UV-Vis and fluorescence spectra of redox state in solution. (b) The measurement method for UV-Vis spectra of the redox product *in situ*. (c) The measurement method for fluorescence spectra of the redox product *in situ*. (d) The taking pictures method for fluorescence in situ (the pictures in Fig. 2). The arrows showed the measurement direction.

3. The preparation methods of the solid electrofluorochromic device

(1) Materials

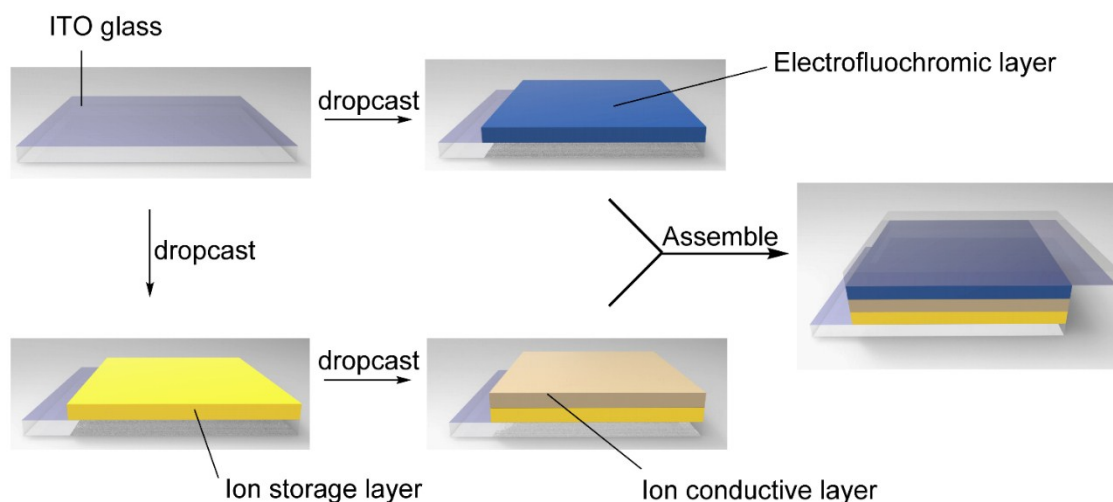
Electrofluorochromic material: A mixture of 0.72 g PMMA, 0.15 ml PC, 0.3 g TBAPF₆, 10.8 mg p-benzoquinone and 0.81 mg 7-hydroxycoumarin in 4 ml CH₃CN was stirred for 3 h at 40 °C, which is used as blue (B) electrofluorochromic layer material. A mixture of 0.72 g PMMA, 0.15 ml PC, 0.3 g TBAPF₆, 10.8 mg p-benzoquinone and 1.94 mg G-OFF molecule in 4 ml CH₃CN was stirred for 3 h at 40 °C, which is used as green (G) electrofluorochromic layer material. A mixture of 0.72 g PMMA, 0.15 ml PC, 0.3 g TBAPF₆, 21.6 mg p-benzoquinone and 2.76 mg R-OFF molecule in 4 ml CH₃CN was stirred for 3 h at 40 °C, which is used as red (R) electrofluorochromic layer material.

Ion storage layer material: A mixture of 1.8 g PMMA, 0.375 ml PC, 0.75 g TBAPF₆, and 46.5 mg ferrocene in 10 ml CH₃CN (10ml CH₂Cl₂ is used to replace CH₃CN for fabricating the solid device R) was stirred for 3 h at 40 °C, which is used as ion storage layer material. To fabricate the encrypted device, the 0.1 g carbon black was added in this ion storage layer material.

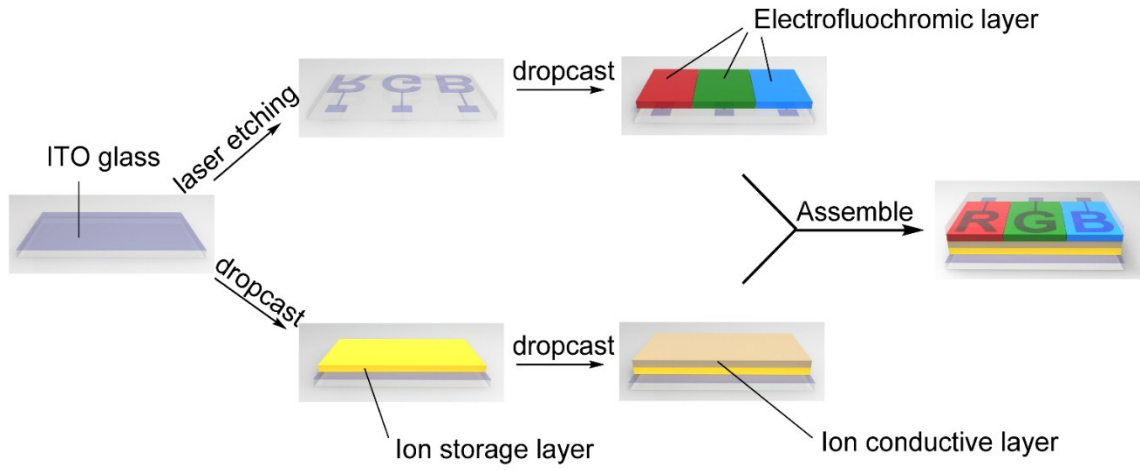
Ion conductive layer material: A mixture of 3.8 g PMMA, 0.75 ml PC, 1.5 g TBAPF₆, in 20 ml CH₃CN (20ml CH₂Cl₂ is used to replace CH₃CN for fabricating fabricate the solid device R) was stirred for 3 h at 40 °C, which is used as ion conductive layer material. To fabricate the encrypted device, the 0.2 g carbon black was added in this ion conductive layer material.

(2) The preparation process of the solid EFC device

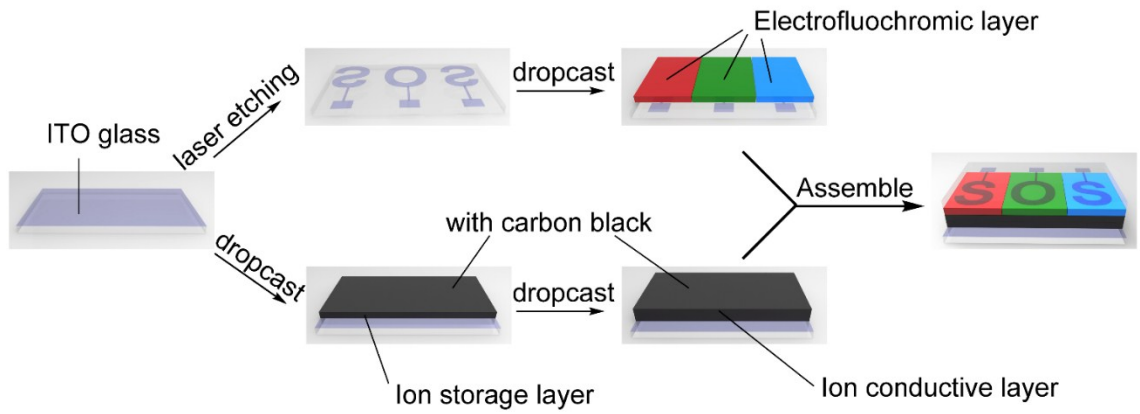
The ITO was etched by laser etching method using a Xi-Ai FB30-Z Laser marking machine.



Scheme S3 The preparation process of single color EFC devices.



Scheme S4 The preparation process of RGB EFC device with displaying RGB letters.



Scheme S5 The preparation process of encrypted RGB EFC device with displaying SOS letters.

4. Synthesis of the G molecule and R molecule

Synthesis of the G molecule (rhodol)¹

2-(4-Diethylamino-2-hydroxybenzyl) benzoic acid (1.253 g, 4.0 mmol) and resorcinol (0.44 g, 4.0 mmol) was dissolved in 15 mL trifluoroacetic acid (TFA) at high-pressure tube, and the mixture react under 90 °C for 12 h. After the reaction finished, the TFA was evaporated under vacuum. The crude product was obtained after dissolving in dichloromethane, washing with the NaHCO₃ aqueous solution, drying with anhydrous sodium sulfate and evaporated. The product was obtained through silica column with dichloromethane/ethyl acetate/methanol (5/5/1) as the eluent to obtain white solid (65%). ¹H NMR (500 MHz, DMSO) δ 10.08 (s, 1H), 7.98 (d, *J* = 6.7 Hz, 1H), 7.78 (t, *J* = 6.5 Hz, 1H), 7.71 (t, *J* = 7.2 Hz, 1H), 7.27 (d, *J* = 6.9 Hz, 1H), 6.68 (s, 1H), 6.53 (s, 2H), 6.46 (d, *J* = 6.0 Hz, 3H), 3.34 (s, 4H), 1.09 (t, *J* = 7.1 Hz, 6H). ¹³C NMR (126 MHz, DMSO) δ = 169.25, 159.85, 152.91, 152.79, 152.66, 149.65, 135.87, 130.39, 129.45, 129.07, 127.00, 124.94, 124.53, 112.75, 110.42, 108.96, 105.24, 102.67, 97.43, 84.44, 44.23, 12.80. LC-HRMS: *m/z* 388.1542 [M+H]⁺, calculated 388.1543. Melting point: 182 °C –183 °C.

Synthesis of the R molecule (2-(2-(4-hydroxystyryl)-6-methyl-4H-pyran-4-ylidene)malononitrile)²

(2,6-Dimethyl-4H-pyran-4-ylidene)malononitrile (1.03 g, 6 mmol), 4-hydroxybenzaldehyde (0.37 g, 3 mmol), piperidine (0.5 ml), acetic acid (0.25 ml) was added in 30 ml methylbenzene. The mixture was refluxed for 8 h under Ar atmosphere. After removal of the solvent, the residue was purified through column chromatography (dichloromethane:ethyl acetate = 30:1 v/v) and recrystal using ethyl acetate and n-hexane to get a yellow solid (51 %). ¹H NMR (500 MHz, DMSO) δ 10.06 (s, 1H), 7.55 (d, *J* = 7.9 Hz, 2H), 7.45 (d, *J* = 16.0 Hz, 1H), 7.11 (d, *J* = 16.0 Hz, 1H), 6.88 – 6.76 (m, 3H), 6.65 (s, 1H), 2.44 (s, 3H). ¹³C NMR (126 MHz, DMSO) δ = 164.39, 160.95, 160.22, 157.19, 138.32, 130.46, 126.43, 116.43, 116.05, 115.88, 106.39, 106.16, 55.53, 19.85. LC-HRMS: *m/z* 277.0971 [M+H]⁺, calculated 277.0972. The melting point is higher than carbonization temperature (280°C), so the melting point can't be measured.

5. pH-sensitive fluorescence properties in solution

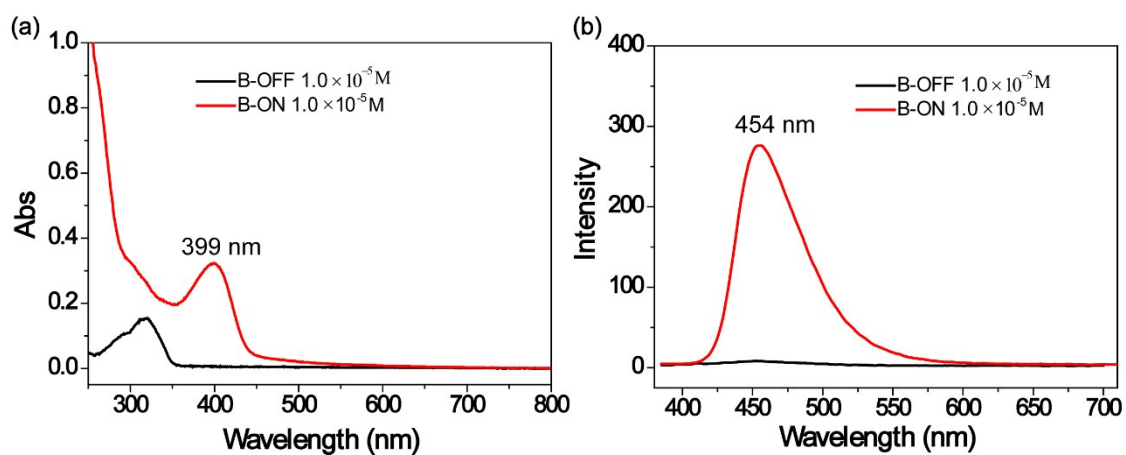


Fig. S1 The UV-Vis spectra (a) and fluorescence spectra (b) of the B molecule (1.0×10^{-5} M) before (black curve, defined as B-OFF) and after (red curve, defined as B-ON) adding 100 eq. t-BuONa in CH₃CN. Excited by 365 nm.

The Fig. S1 shows that the solution of the **B** molecule could be switched from no fluorescence to strong blue fluorescence by adding base.

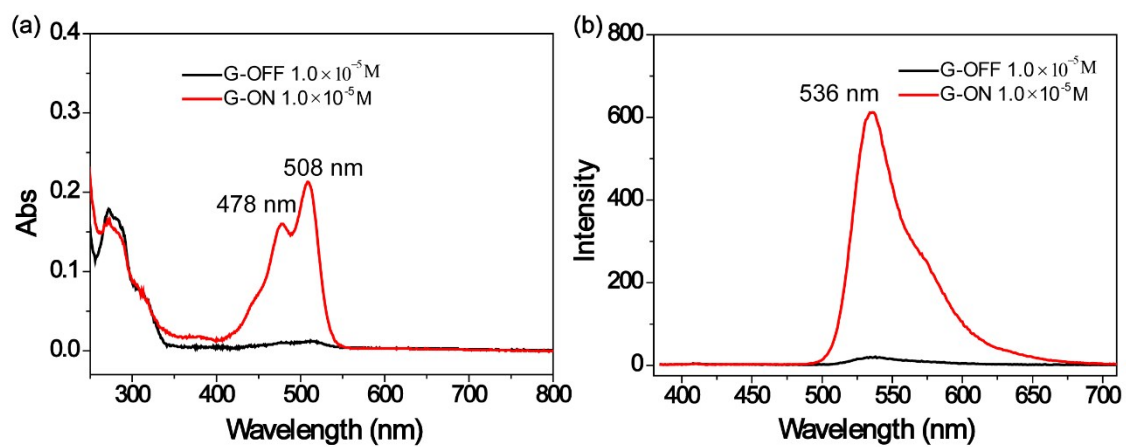


Fig. S2 The UV-Vis spectra (a) and fluorescence spectra (b) of the G molecule ($1.0 \times 10^{-5} \text{ M}$) before (black curve, defined as G-OFF) and after (red curve, defined as G-ON) adding 100 eq. t-BuONa in CH_3CN . Excited by 365 nm.

The Fig. S2 shows that the solution of the **G** molecule could be switched from no fluorescence to strong green fluorescence by adding base.

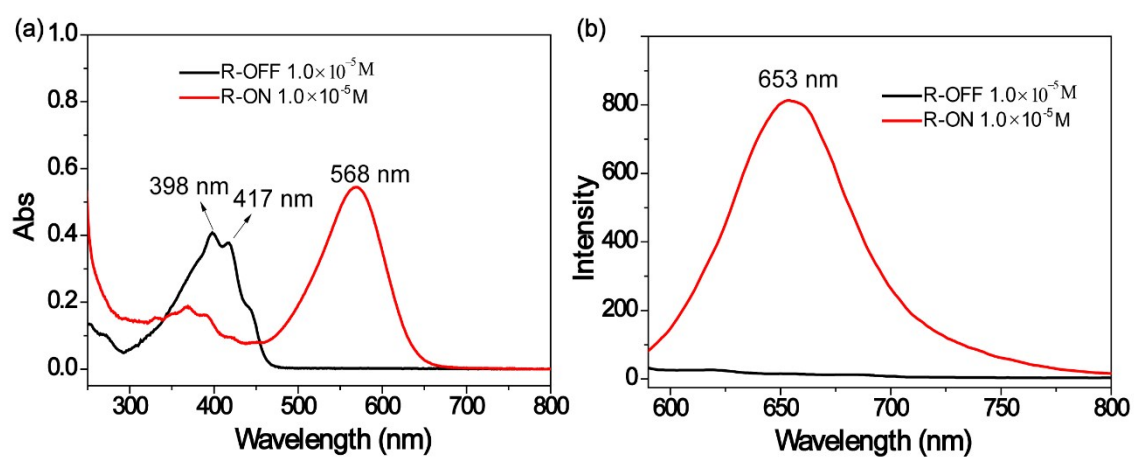


Fig. S3 The UV-Vis spectra (a) and fluorescence spectra (b) of the **R** molecule (1.0×10^{-5} M) before (black curve, defined as R-OFF) and after (red curve, defined as R-ON) adding 100 eq. *t*-BuONa in CH_3CN . Excited by 570 nm.

The Fig. S3 shows that the solution of the **R** molecule could be switched from no fluorescence to strong red fluorescence by adding base.

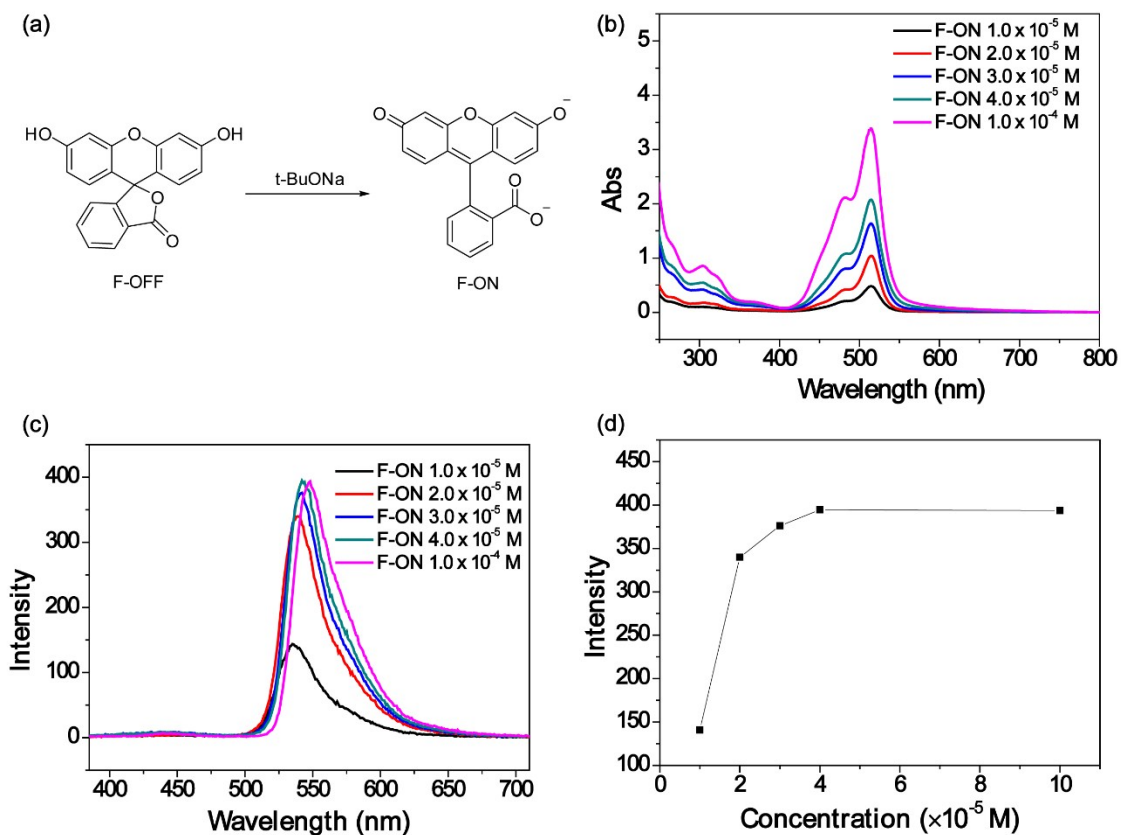


Fig. S4 (a) The structure changing of the fluorescein induced by t-BuONa. (b) The UV-Vis spectra of fluorescein at different concentrations with t-BuONa (1.0×10^{-3} M). (c) The fluorescence spectra of fluorescein at different concentrations with t-BuONa (1.0×10^{-3} M). (d) The fluorescence intensity changing with concentration.

The **F** molecule (**Fluorescein**) was used in our previous work³ to demonstrate the feasibility of electrofluorochromism based on electro-base mechanism. With the concentration of the **F-ON** molecule increasing, the absorption increases, while the fluorescence increases at low concentration and decreases at high concentration (Fig. S4). It is because the fluorescence of **F-ON** molecule is easily to quench at high concentration (4.0×10^{-5} M according to the Fig. S4d). This phenomenon would influence the performance of the EFC device.

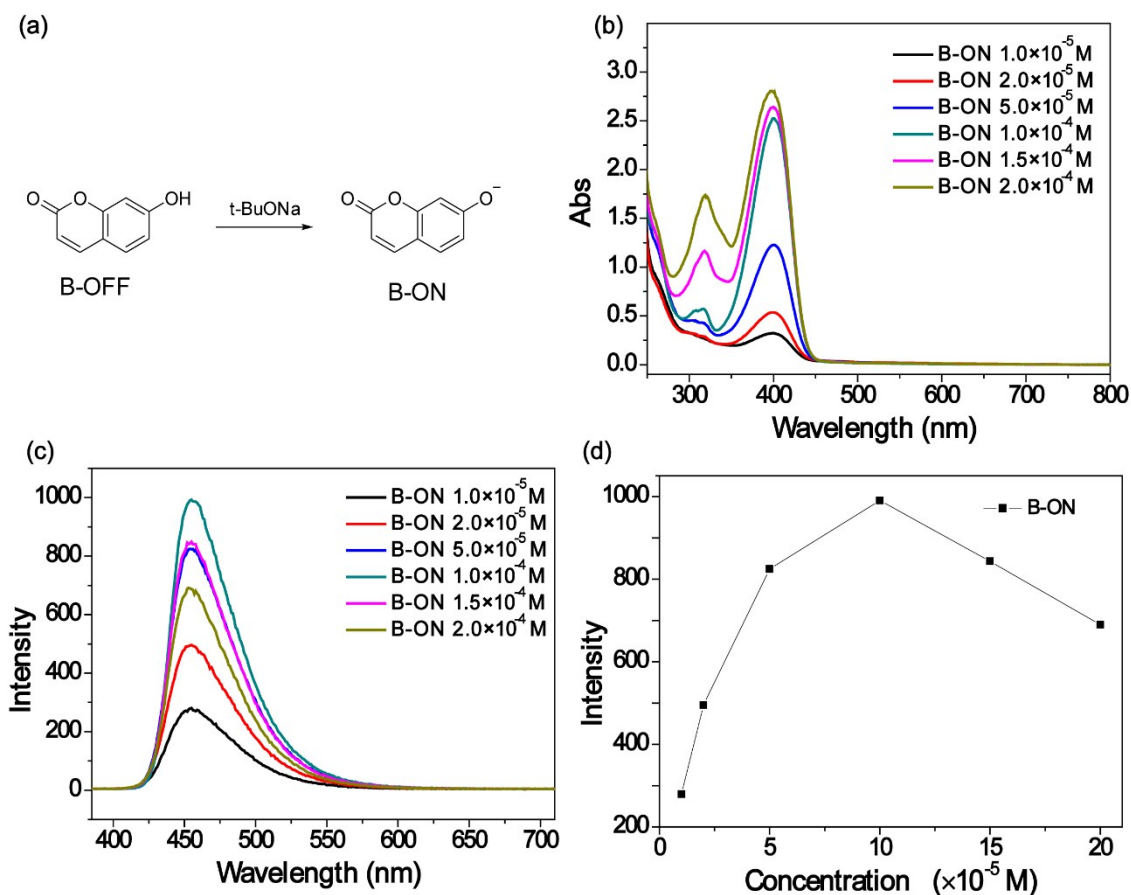


Fig. S5 (a) The structure changing of **B** molecule stimulated by base t-BuONa. (b) The UV-Vis spectra of **B-ON** at different concentrations with t-BuONa (1.0×10^{-3} M). (c) The fluorescence spectra of **B-ON** at different concentration with t-BuONa (1.0×10^{-3} M). (d) The fluorescence intensity changing with concentration.

With the concentration of the **B-ON** molecule in solution increasing, the absorption of the solution increases, while the fluorescence increases at low concentration and decreases at high concentration (Fig. S5). The trend is same with the **F-ON** molecule. However, **B-ON** molecule needs higher concentration when its fluorescence is quenched (1.0×10^{-4} M according to Fig. S5d) compared with **F** molecule. That is to say, higher concentration of **B** molecule can be used in solid EFC device for obtaining a high fluorescence intensity.

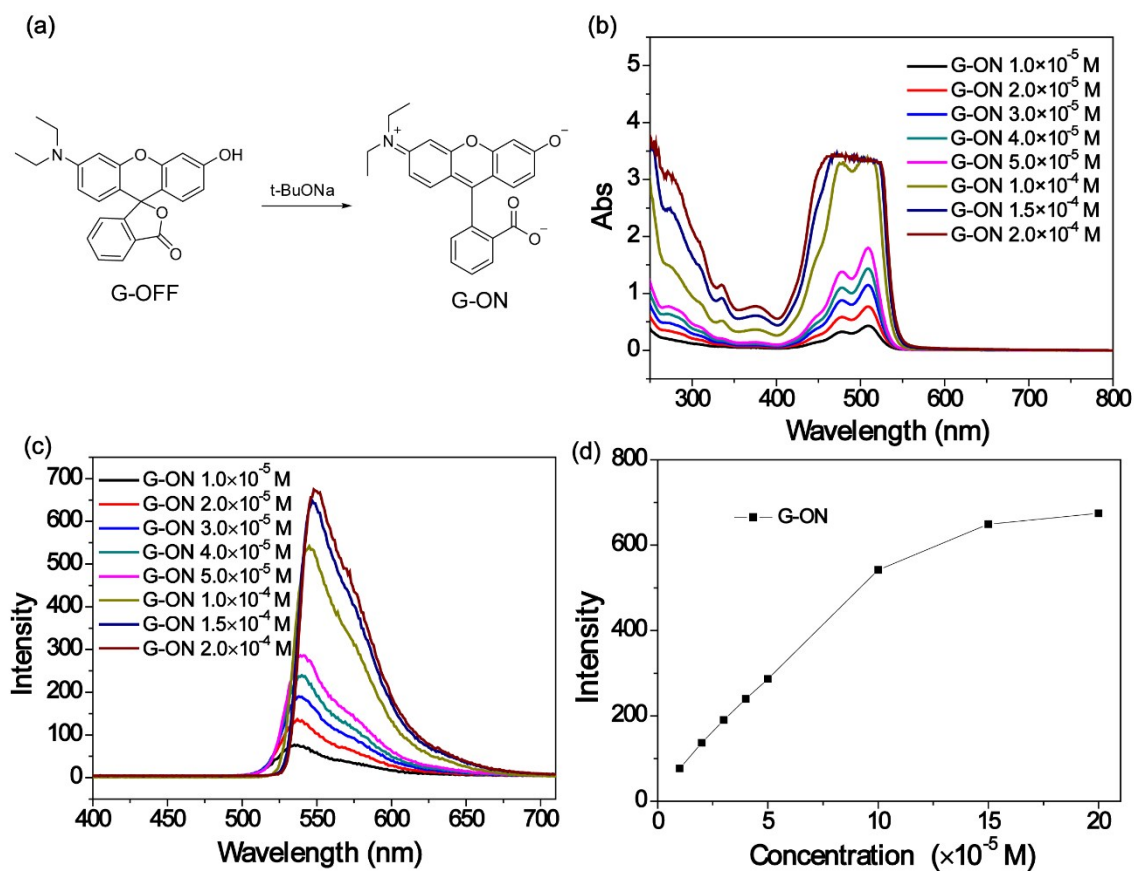


Fig. S6 (a) The structure changing of **G** molecule stimulated by base t-BuONa. (b) The UV-Vis spectra of **G-ON** at different concentration with t-BuONa (1.0×10^{-3} M). (c) The fluorescence spectra of **G-ON** at different concentration with t-BuONa (1.0×10^{-3} M). (d) The fluorescence intensity changing with concentration.

With the concentration of the **G-ON** molecule in solution increasing, the absorption and fluorescence of the solution both increase according to Fig. S6. It demonstrates that the fluorescence of the **G-ON** molecule is not easy to be quench at high concentration.

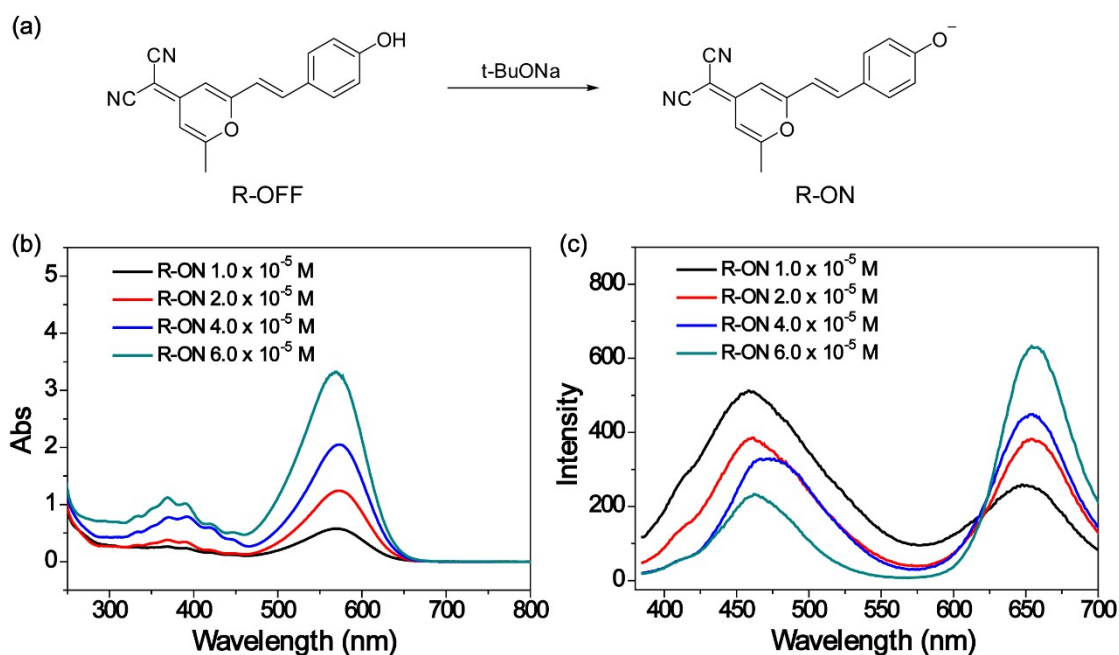


Fig. S7 (a) The structure changing of the **R** molecule stimulated by base t-BuONa. (b) The UV-Vis spectra of the **R-ON** at different concentration with t-BuONa (1.0×10^{-3} M). (c) The fluorescence spectra of **R-ON** at different concentration with t-BuONa (1.0×10^{-3} M). Excited by 365 nm.

As shown in Fig. S7, with the concentration of the **R-ON** molecule in solution increasing, the absorption at 370 nm and 570 nm both increase. However, the fluorescence of 455 nm decreases along with the fluorescence at 645 nm increasing. This phenomenon is a typical characteristic of the excimer, which demonstrates that the red fluorescence of **R-ON** can be assigned to the excimer of **R-ON** molecule. Thus, the high concentration of **R-ON** will exhibit a high intensity of fluorescence. Considering that **R-ON** molecule has a high solubility in CH_3CN , it is difficult to form excimer. So CH_2Cl_2 solvent is used to fabricate the solid device for obtaining stronger fluorescence.

6. Spectroelectrochemical measurements *in situ*

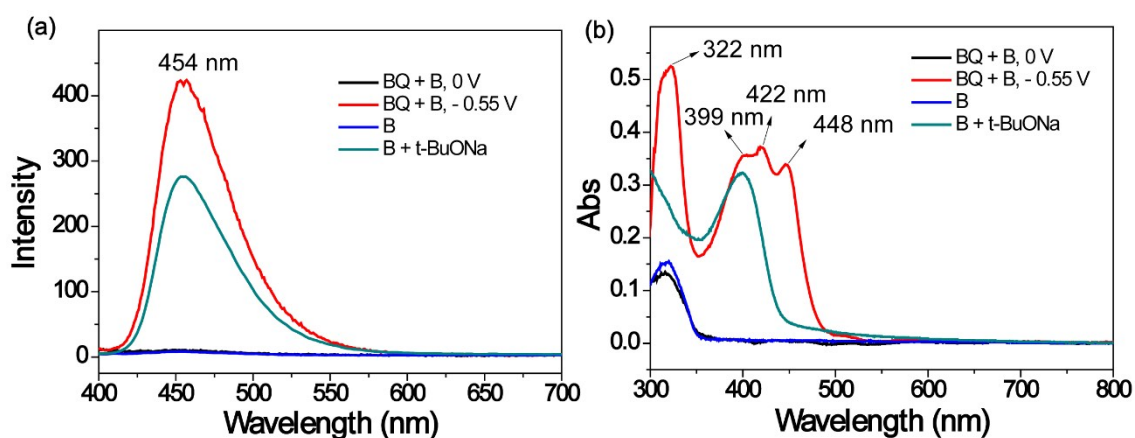


Fig. S8 (a) The fluorescence spectroelectrochemical spectra *in situ* of mixture of **p-BQ** (1.0×10^{-3} M) and **B** (1.0×10^{-4} M) in CH_3CN with 0.1 M TBAPF₆ when the voltage is set as 0 V and -0.55 V, respectively. And the fluorescence spectra of **B** molecule solution (1.0×10^{-5} M) and **B** solution (1.0×10^{-5} M) with 100 eq. t-BuONa in CH_3CN . (b) The UV-Vis spectroelectrochemical spectra *in situ* of mixture of **p-BQ** (1.0×10^{-3} M) and **B** (1.0×10^{-4} M) in CH_3CN with 0.1 M TBAPF₆ when the voltage is set as 0 V and -0.55 V, respectively. And the UV-Vis absorption spectra of **B** molecule solution (1.0×10^{-5} M) and **B** solution (1.0×10^{-5} M) with 100 eq. t-BuONa in CH_3CN .

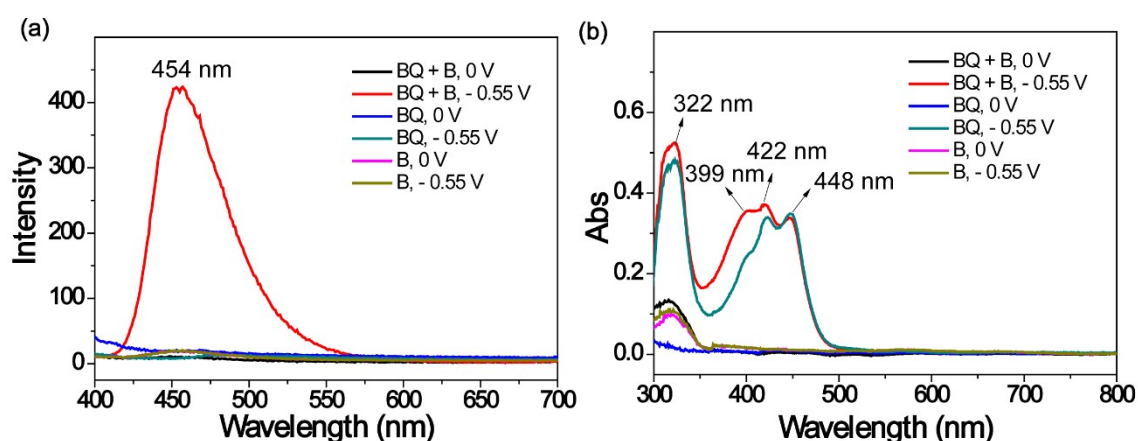


Fig. S9 (a) The fluorescence spectroelectrochemical spectra *in situ* and (b) the UV-Vis spectroelectrochemical spectra *in situ* of mixture of **p-BQ** (1.0×10^{-3} M) and **B** (1.0×10^{-4} M), and individual **p-BQ** (1.0×10^{-3} M), and individual **B** (1.0×10^{-4} M) in CH_3CN with 0.1 M TBAPF₆ when the voltage is set as 0 V and -0.55 V, respectively.

No fluorescence can be observed when the -0.55 V voltage was applied on the individual **p-BQ** and individual **B** (Fig. S9). Only for the mixture of **p-BQ** and **B**, the fluorescence can be observed when the -0.55 V voltage was applied. When -0.55 V voltage was applied, the absorption spectrum of individual **B** molecule shows no change. However, when the voltage was applied on the mixture of **p-BQ** and **B**, a new peak appeared which is different with **p-BQ**^{•-} generated by applied -0.55 V (Fig. S9). The new peak is same with the base-form **B** stimulated by t-BuONa (Fig. S8). And the position of generated fluorescence of the mixture of **p-BQ** and **B** is also same with base-form **B**. This indicates that **B** molecule is stimulated by the electro-base, reduced **p-BQ**. The similar phenomenon is also seen for **G** and **R** molecules as shown in Fig. S10, S11, S12 and S13.

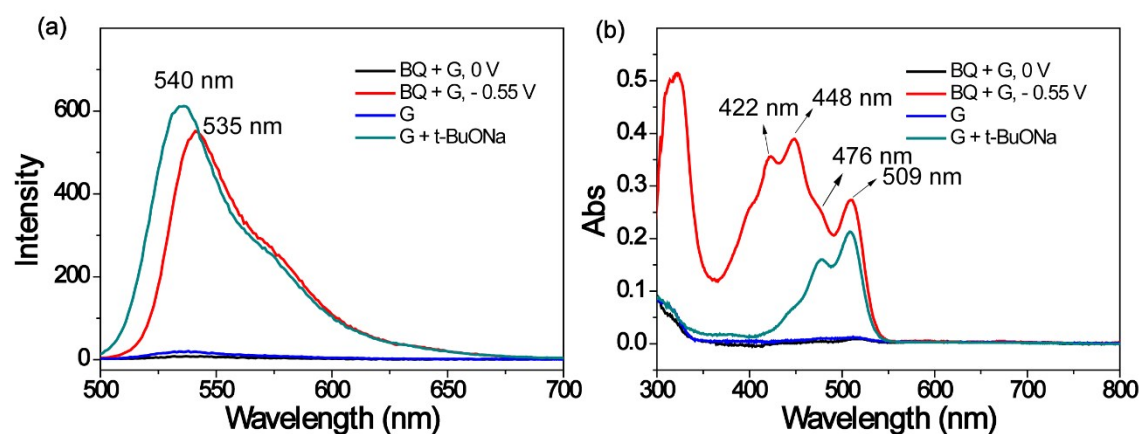


Fig. S10 (a) The UV-Vis spectroelectrochemical spectra *in situ* of mixture of **p-BQ** (1.0×10^{-3} M) and **G** (1.0×10^{-4} M) in CH_3CN with 0.1 M TBAPF_6 when the voltage is set as 0 V and -0.55 V, respectively. And the UV-Vis absorption spectra of **G** molecule solution (1.0×10^{-5} M) and **G** solution (1.0×10^{-5} M) with 100 eq. t-BuONa in CH_3CN . (b) The fluorescence spectroelectrochemical spectra *in situ* of mixture of **p-BQ** (1.0×10^{-3} M) and **G** (1.0×10^{-4} M) in CH_3CN with 0.1 M TBAPF_6 when the voltage is set as 0 V and -0.55 V, respectively. And the fluorescence spectra of **G** molecule solution (1.0×10^{-5} M) and **G** solution (1.0×10^{-5} M) with 100 eq. t-BuONa in CH_3CN .

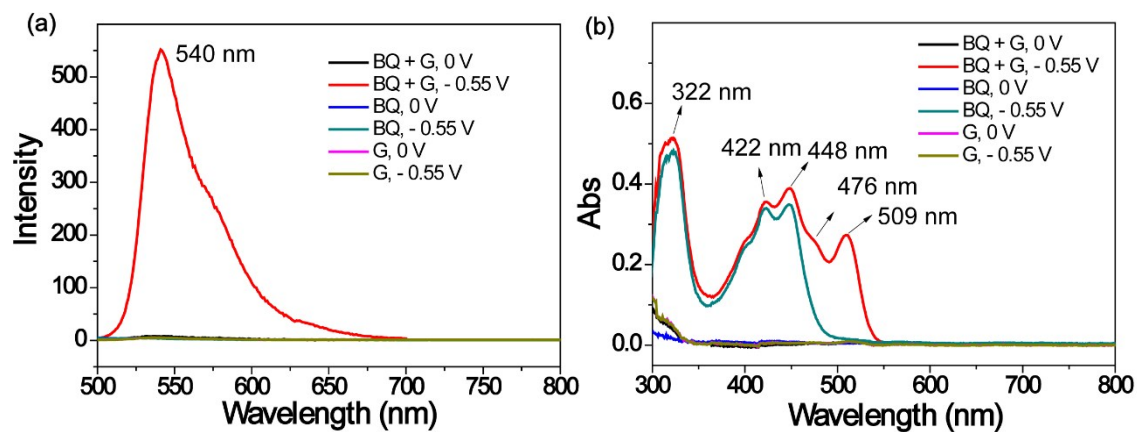


Fig. S11 (a) The UV-Vis spectroelectrochemical spectra *in situ* and (b) the fluorescence spectroelectrochemical spectra *in situ* of mixture of **p-BQ** (1.0×10^{-3} M) and **G** (1.0×10^{-4} M), and individual **p-BQ** (1.0×10^{-3} M), and individual **G** (1.0×10^{-4} M) in CH_3CN with 0.1 M TBAPF_6 when the voltage is set as 0 V and -0.55 V, respectively.

The slight red shift of the fluorescence peak of **G** induced by electro-base (540 nm), compared with stimuli of chemical base (535 nm) is due to the difference in concentration of **G-ON** according to the Fig. S6c. The fluorescence peak of **G-ON** exhibited a red shift with the concentration increasing.

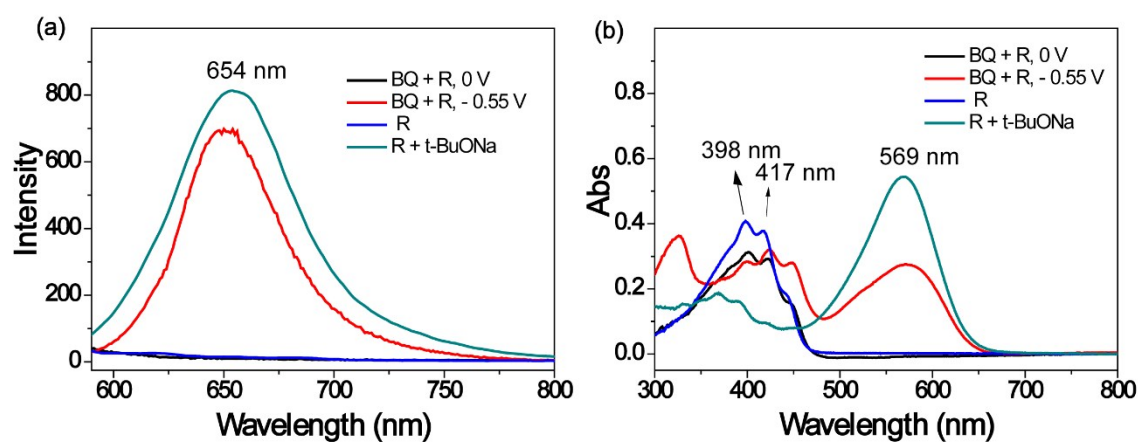


Fig. S12 (a) The UV-Vis spectroelectrochemical spectra *in situ* of mixture of p-BQ (1.0×10^{-3} M) and R (1.0×10^{-4} M) in CH_2Cl_2 with 0.1 M TBAPF₆ when the voltage is set as 0 V and -0.55 V, respectively. And the UV-Vis absorption spectra of R molecule solution (1.0×10^{-5} M) and R solution (1.0×10^{-5} M) with 100 eq. t-BuONa in CH_3CN . (b) The fluorescence spectroelectrochemical spectra *in situ* of mixture of p-BQ (1.0×10^{-3} M) and R (1.0×10^{-4} M) in CH_2Cl_2 with 0.1 M TBAPF₆ when the voltage is set as 0 V and -0.55 V, respectively. And the fluorescence spectra of R molecule solution (1.0×10^{-5} M) and R solution (1.0×10^{-5} M) with 100 eq. t-BuONa in CH_3CN .

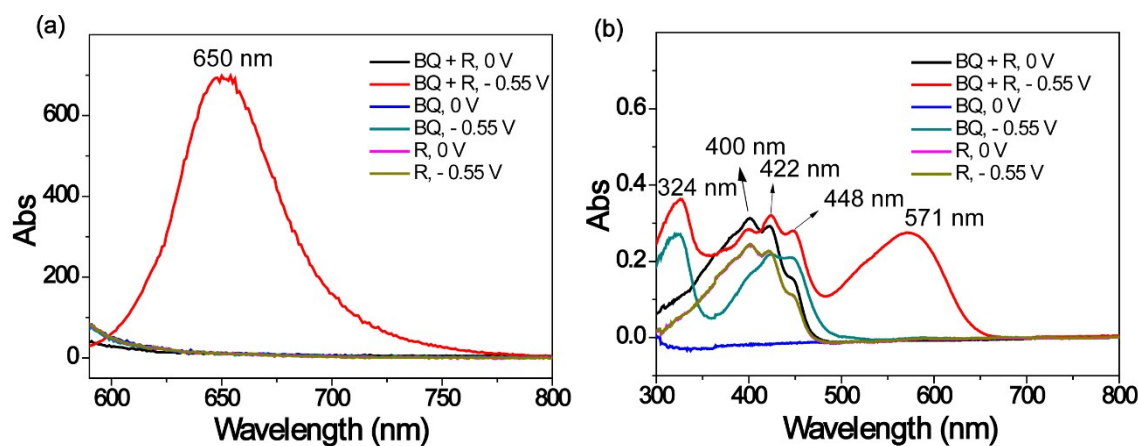


Fig. S13 (a) The UV-Vis spectroelectrochemical spectra *in situ* and (b) the fluorescence spectroelectrochemical spectra *in situ* of mixture of p-BQ (1.0×10^{-3} M) and R (1.0×10^{-4} M), and individual p-BQ (1.0×10^{-3} M), and individual R (1.0×10^{-4} M) in CH_2Cl_2 with 0.1 M TBAPF₆ when the voltage is set as 0 V and -0.55 V, respectively.

7. Supplementary Figures for solid devices

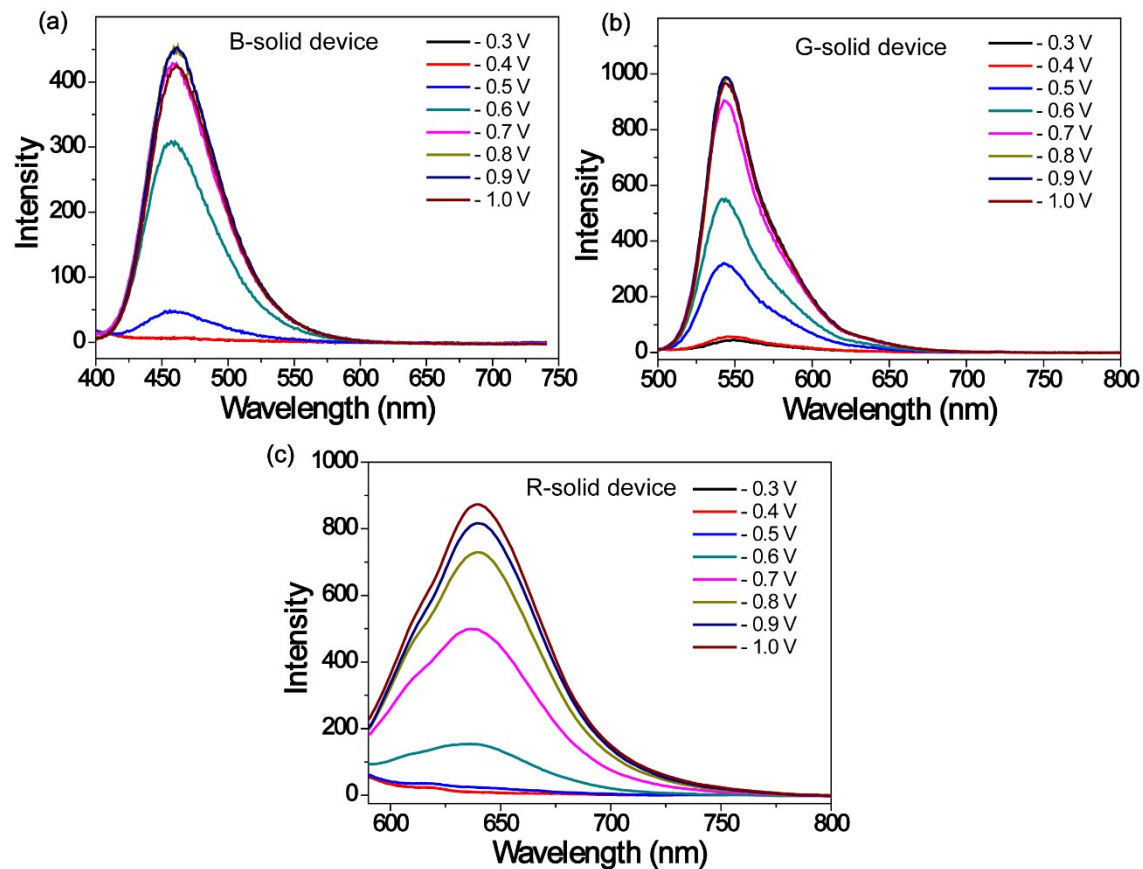


Fig. S14 The fluorescence spectra of B (a), G (b) and R (c) solid devices without carbon black under different voltage.

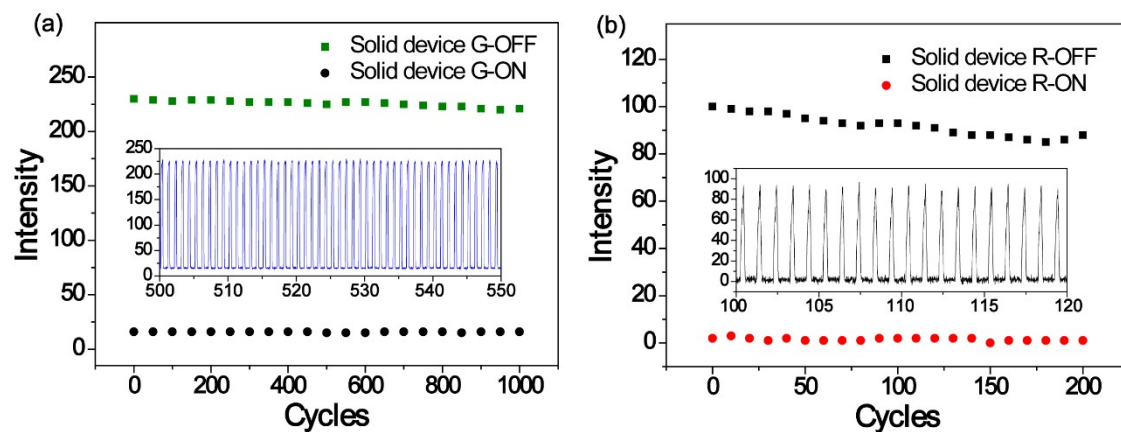


Fig. S15 The reversibility of G (a) and R (b) solid devices stimulated by -1.0 V/+0.3 V, repeatedly.

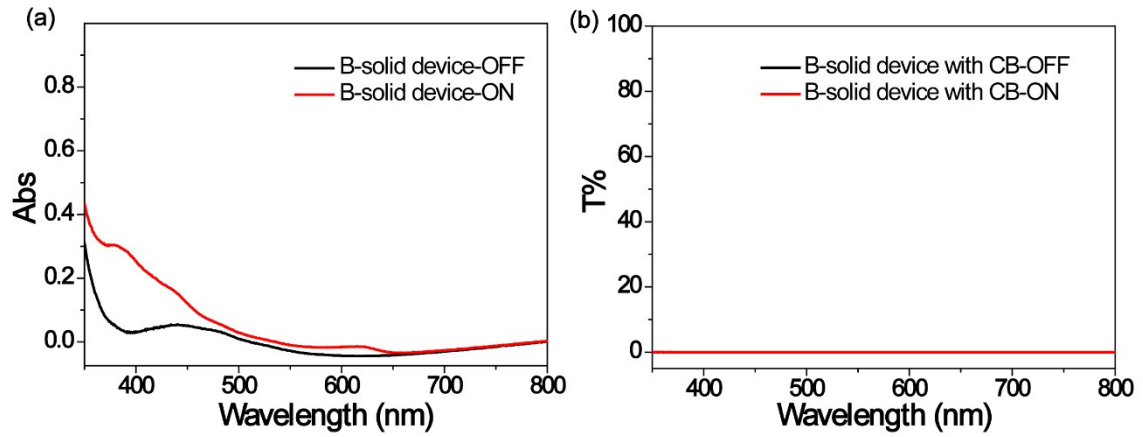


Fig. S16 (a) The absorption spectra of **B** solid device at OFF and ON states without carbon black. (b) The absorption spectra of encrypted **B** solid device at OFF and ON states with carbon black in ion storage layer and ion conductive layer.

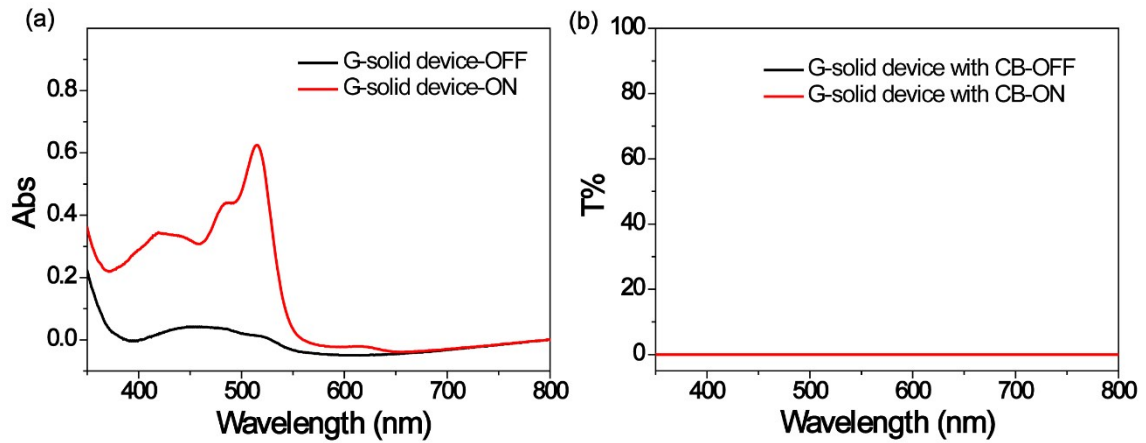


Fig. S17 (a) The absorption spectra of **G** solid device at OFF and ON states without carbon black. (b) The absorption spectra of encrypted **G** solid device at OFF and ON states with carbon black in ion storage layer and ion conductive layer.

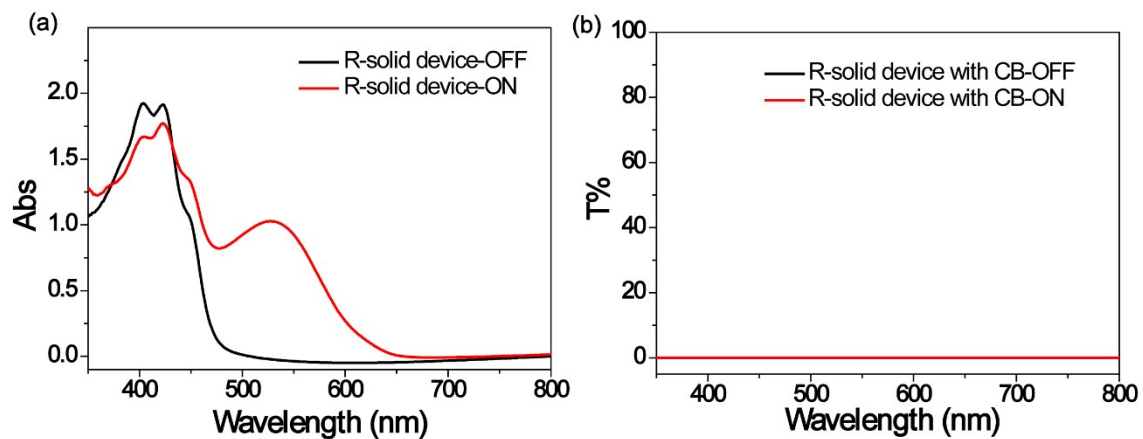


Fig. S18 (a) The absorption spectra of R solid device at OFF and ON states without carbon black. (b) The absorption spectra of encrypted R solid device at OFF and ON states with carbon black in ion storage layer and ion conductive layer.

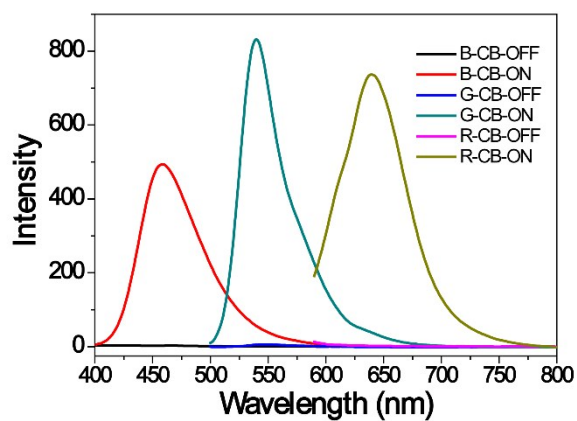


Fig. S19 (a) The fluorescence spectra of encrypted solid devices at OFF and ON states with carbon black in ion storage layer and ion conductive layer.

8. NMR spectra.

Fig. S20 NMR spectra of G molecule.

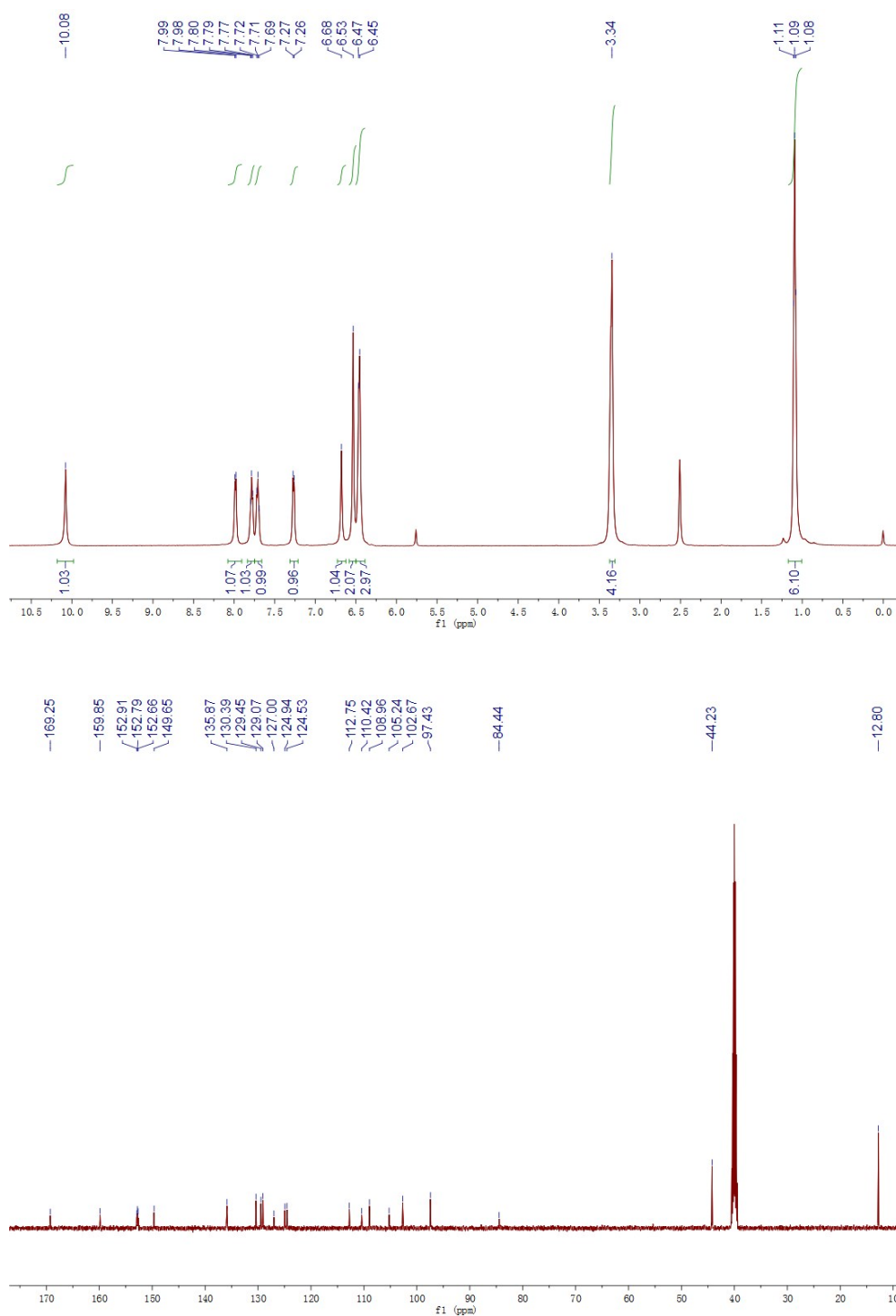
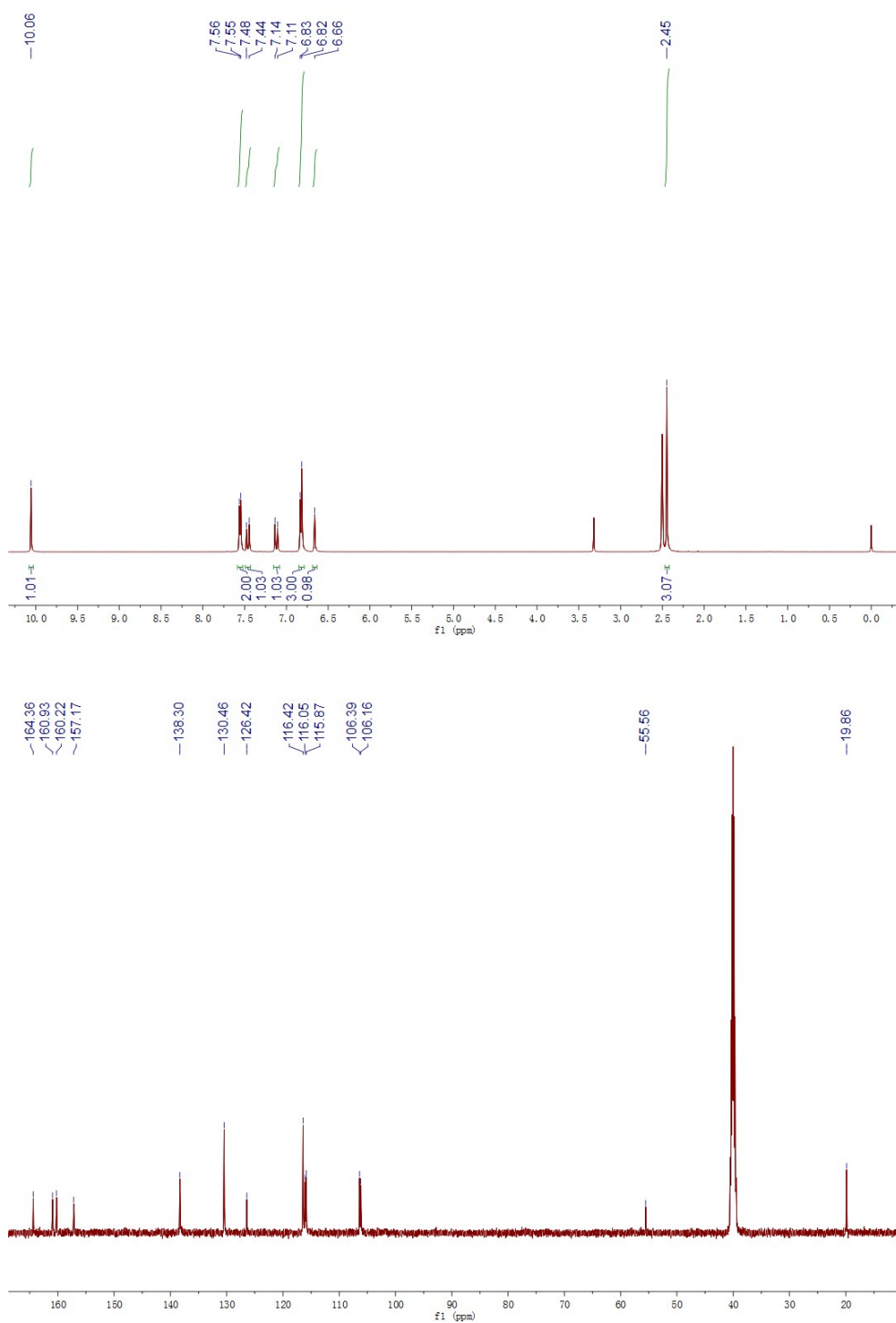


Fig. S21 NMR spectra of R molecule.



9. References

1. B. C. Dickinson, C. Huynh, C. J. Chang, *J. Am. Chem. Soc.*, 2010, **132**, 5906-5915.
2. Z. Guo, P. Zhao, W. Zhu, X. Huang, Y. Xie, H. Tian, *J. Phys. Chem. C*, 2008, **112**, 7047-7053.
3. Y. M. Zhang, W. Li, X. Wang, B. Yang, M. Li, S. X. Zhang, *Chem. Commun.*, 2014, **50**, 1420-1422.